2019 IEEE Intelligent Vehicles Symposium (IV)
Paris, France. June 9-12, 2019

Modelling the dynamic behavior of the steering system for low speed autonomous path tracking

Ádám Domina, Viktor Tihanyi

Abstract—**In the future, the appearance of highly automated vehicles is expected, the driver assistance systems will become more common in the vehicles. Initially, these systems are only supported the driver, but increasingly take over the control of the entire vehicle. In this practice, the vehicle must plan the route and follow it safely while providing a comfortable journey for passengers. In order to develop the path following controller, it is first tested in a simulation environment and then on a real vehicle.**

In a previous paper, authors have implemented different path following controllers that were tested on a demonstration vehicle after testing in the simulation environment. In the simulation environment, the controllers were tested on a dynamic bicycle model, which model describes the lateral dynamics of the vehicle. The simulation and measurement results showed a difference. The subject of this paper is to find out the reason of the difference that was identified in the dynamic behavior of the steering system, including the effect of the tires. Based on these, the vehicle model was adjusted. Measurements were made to identify the dynamics of the steering system, and the tires. Analyzing the results of the measurements, the dynamic model of the steering system was described, the vehicle model has been expanded on this basis.

Finally, the path following simulation with the improved model was calculated, which was compared to the real vehicle measurement and the results showed good correlation.

I. Introduction

In recent years, vehicle manufacturers are increasingly focusing on vehicles with automated systems. The driver performs an extremely complex task during driving, actually available driver assistant system below level 3 according to SAE levels provide support for the drivers to decrease their load. These systems improve road safety, eco-friendliness, efficiency, comfort, reduce travel times and pollutant emissions. Global transport challenges such as the increasing traffic density resulting from urbanization, the reduction of accidents, and the improvement of energy efficiency all benefit the development of automated vehicles. To achieve these goals, highly automated road vehicles, intelligent road infrastructure and automated transport organization are needed together.

In order to achieve these improvements, it is necessary to increase the level of automation of the vehicles on the one hand and to develop the intelligent infrastructure and transport environment on the other. A good example of this is the appearance of smart city and V2X communication, in the latter case the vehicle communicates with the other vehicle or with intelligent elements of the transport infrastructure.

The autonomous vehicles in the future will have to perform complex control operation keeping the vehicle on the road. There are a lot of effects to be considered in order to develop such a complex system. Because it is a very difficult task to prepare for all possible scenarios developing and testing such systems is a major challenge for developers [1], [2].

The automated vehicle control hierarchy consists of four layers. These are the driver interface layer, the environment perception layer, the command layer, and the executing layer. The driver interface layer is responsible for conducting human-machine interaction. The environment perception layer monitors the ever-changing environment of the vehicle, recognizes the objects, obstacles, traffic participants, horizontal and vertical traffic signs [3] that are there. The command layer makes decision-making and path planning processes based on the data which have collected from the other layers. The executive layer is responsible for the longitudinal and lateral control of the vehicle, and executes the instructions received from the command layer. The path following algorithms that are the subject of this paper belong to this layer.

The subject of this paper is the development of path following controllers. First, the algorithms are tested in a simulation environment using a vehicle model and the controller for tuning it. Realistic modeling is essential during this phase otherwise the controller algorithm will behave completely different in the real vehicle environment. This is the development process of a controller [5]. The advantage of the software simulation is that the controllers can be easily tuned in the software environment and, if they work properly, can be tested on a real vehicle, saving time and resources. The more sophisticated the vehicle model, the more the simulation results will be closer to the measurement results. In the previous paper [4], the authors have implemented three path following controllers [6], [7], [8] and then tested them in a dynamic bicycle model in a software environment. After the controllers functioned properly in the simulation, they were tested on a real vehicle. The tests showed a difference from the simulation results due to neglecting many dynamic aspects of the real vehicle that have significant impact on the behavior. As the speed was increased, the difference between the simulated and the real vehicle motion characteristics was getting higher. At higher speeds the real vehicle started to

Á. D. Author is with the Department of Automotive Technologies, Budapest University of Technology and Economics, Budapest, 1111 Hungary (e-mail: adam.domina@gjt.bme.hu).

V. T. Author is with the Department of Automotive Technologies, Budapest University of Technology and Economics, Budapest, 1111 Hungary (e-mail: viktor.tihanyi@gjt.bme.hu).

oscillate around the path while in the simulation the speed value had no influence.

This paper is a continuation of the authors' previous paper, focusing on the evaluation of the differences between real vehicle and lateral dynamic bicycle model. In this article, the already existing and commonly used mentioned model [8], [9], [10], [11], [12] has been upgraded with dynamics of the steering system and tires.

II. SMART DEMONSTRATION VEHICLE AND IMPROVED VEHICLE MODEL

"Fig. 1" shown the Smart demonstration vehicle. The Department of Automotive Technologies at the Budapest University of Technology and Economics is constantly making improvements on the vehicle to achieve the highest level of automation. The demonstration vehicle is suited for performing tests for validating research results in practice.

The vehicle equipped with dSpace Autobox, which is responsible for vehicle control, camera, LIDAR and RADAR sensors, and two high precision GNSS systems. The two GNSS are required for having redundancy, if one does not work with sufficient accuracy, the other can still define the vehicle's position. This is essential for path following, which is based on GNSS positioning.

A dynamic bicycle model was used for the simulation results [4], the upper limit of the applicability of the simulations based on the measurements was 15 km/h.

Figure 1. Smart demonstration vehicle.

At higher speeds, there was a significant difference between simulation and reality. Path tracking in the simulation remained accurate, in reality the vehicle deviated significantly from the track. There are two typical defective movements. One is the oscillating movement of the vehicle along the path. Another is the vehicle overshoot when arriving at the curves. The overshoot occurs when the vehicle is starting the cornering operation just after reaching the place of the turn in the path. The reason for the difference between reality and simulations is the neglect of more dynamic phenomena. The inertia and resistance of the steering system should be considered – that is typically taken into account with a single time constant [13], or with yaw damping [14], [15] – and the dynamic behavior of tires, without this the simulated vehicles steering angle is reached without any delay from the reference value. If the steering angle requested by the path following controller is delayed, then the vehicle will cornering later than necessary, which explains the overshoot and oscillation differences. The vehicle model used is described by two equations:

$$\dot{v}_y = \frac{-c_f\left[tan^{-1}\left(\frac{v_y + l_f\omega}{v_x}\right) - \delta\right]cos(\delta) - c_r\, tan^{-1}\left(\frac{v_y - l_r\omega}{v_x}\right)}{m} - v_x\omega \quad (1)$$

$$\dot{\omega} = \frac{-l_f c_f\left[tan^{-1}\left(\frac{v_y + l_f\omega}{v_x}\right) - \delta\right]cos(\delta) + l_r c_r\, tan^{-1}\left(\frac{v_y - l_r\omega}{v_x}\right)}{I_z} \quad (2)$$

where v_y is the lateral velocity of the vehicle, c_f and c_r are the cornering stiffness of the front and the rear tires, l_f and l_r are the distance between the center of gravity of the vehicle (C.G.) and the front and rear axles. δ is the steering angle, ω is the yaw-rate of the vehicle, v_x is the longitudinal velocity of the vehicle, m is the mass of the vehicle and I_z is the inertia of the vehicle along the z-axis. The longitudinal dynamics of the vehicle has been neglected, this is not necessary due to constant speed going, and this would only have an effect on stopping and starting. During the measurements, the vehicle started before the track, when it arrived at the track, accelerated to the desired speed. In all cases, the measurements were stopped after reaching the last point of the track. This means that adjusting the value of v_x to constant in the simulation did not cause any difference between simulation and measurement. The equations are complemented by a third equation describing the dynamics of steering:

$$M_{mot} = M_{tire} * i_{cw} + M_{sa} * i_{cw} + \Theta * \ddot{\delta} \quad (3)$$

where M_{mot} is the torque generated by the electric steering servo motor. M_{tire} is the steering resistant torque which prevents the wheels from rotating around its vertical axis (z-axis) of rotation through the rubber asphalt frictional connection. M_{sa} is the self-aligning torque, generated by the pneumatic trail of the tire, i_{cw} is the wheel-column transmission ratio in the steering system. Θ is the inertia of the steering system, including the column, pinion, rack, hub and the wheels, reduced to the steering column. $\ddot{\delta}$ is the angular acceleration of the steering column. The torques described are a function of several factors, in the following, these torques will be defined.

A. The inertia of the steering system

Knowledge of the value of the inertia of the steering system (Θ) is required to create the model of the steering system [17]. Θ can be determined if the value of M_{tire} and M_{sa} in (3) is zero. This occurs when the vehicle is moving at zero speed and there is no friction between the tire and the ground. M_{tire} is zero due to zero speed, M_{sa} is zero due to lack of friction. This condition occurs when the car is lifted up. Hence, the vehicle was lifted up, and measurements were made to calculate the value of Θ. In this state of the vehicle (3) can be simplified to (4).

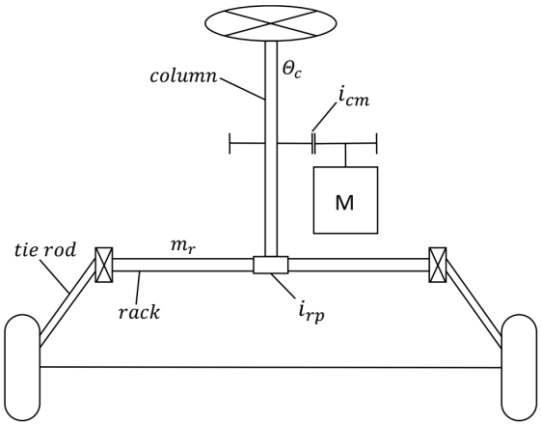

Figure 2. Kinematic model of the steering system.

$$M_{mot} = \Theta * \ddot{\delta} \tag{4}$$

The steering angle (δ) and electric steering servo engine torque (M_{mot}) are recorded on the steering column during measurements, consider M_{mot} is not the torque on the electric motor shaft, but the torque on the steering column. During the measurements, the steering column rotation was measured at the specified torque value. The angular acceleration of the steering column can be calculated by second derivation of δ, knowing this the value of Θ can be calculated from (4). The calculated value of Θ is the total inertia of the entire steering system reduced to the steering column. "Fig. 2" shows the kinematic arrangement of the steering system. The measurement result shows the value of Θ is 0.00345 kg*m^2.

B. *Self-aligning torque*

When the vehicle moves on a curved track, side forces (F_y) affect the vehicle. The side forces are transmitted due the frictional relationship between the tire and ground. The lateral force is at a distance $a_{x\alpha}$ behind the centerline of the tireprint. The distance called pneumatic trail. This creates a torque M_{sa} called self-aligning torque that rotates the wheel around its z axis, and tends to reduce sideslip angle α. "Fig. 3" show the principle of the pneumatic trail.

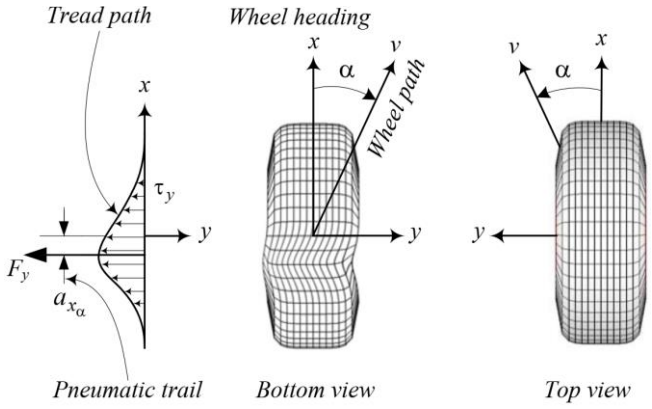

Figure 3. Self-aligning torque as a function of lateral slip. [18]

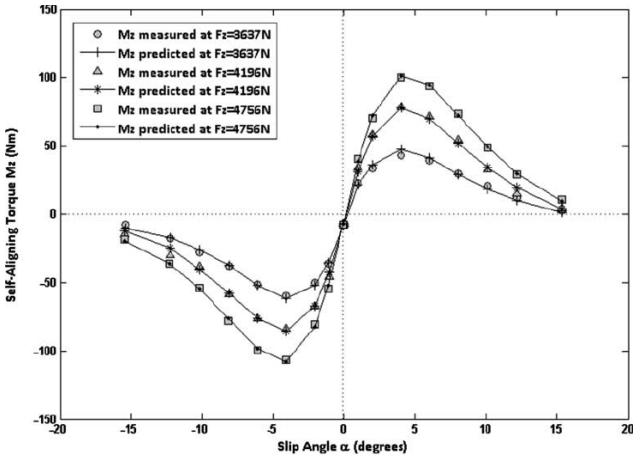

Figure 4. Self-aligning torque as a function of sideslip. [20]

The value of self-aligning torque is tire and vehicle specific, its determination requires a complex measurement system. Therefore it was determined from experimental data, based on the knowledge of sideslip angle. "Fig. 4" shows the used measurement data at different axle loads, the self-aligning torque is a function of sideslip angle. The vehicle model used calculates the sideslip angle, hence M_{sa} can be determine using the diagram in Fig. 4. The front axle load of the Smart is 380 kg, it is close enough to the measurement data of the smallest axle load, that dataset can be used. In Fig. 4 circles marks the corresponding dataset. The diagram defines M_{sa} as a function of steering angle $M_{sa}(\alpha)$.

C. *Steering resistant torque*

This torque assigned M_{tire} in (3) is caused by friction between the tire and the road surface. "Fig. 5" shows the contact surface and the principle of calculating steering resistant torque.

The steering resistant torque is the function of the vehicle speed. The torque magnitude is inversely proportional to speed, more the faster the vehicle moves, the lower its value. Is the highest when the vehicle speed is zero.

On "Fig. 5" F is the circumferential forces, it has been generated at each dA element, at the belonging radius r. F can be calculated from the normal force F_z, knowing the friction factor μ, F= μ*F_z. To calculate M_{tire}, F must be integrated across the entire contact area, according to (5) [20].

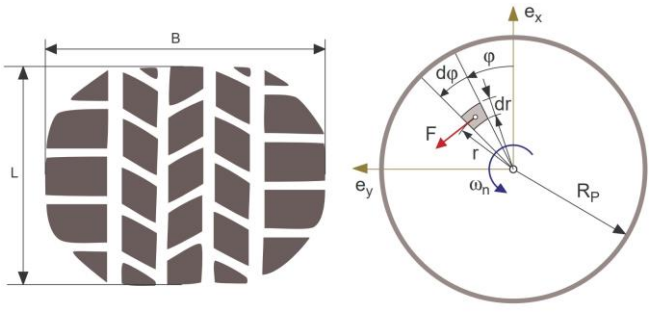

Figure 5. Approximation of the steering resistant torque. [19]

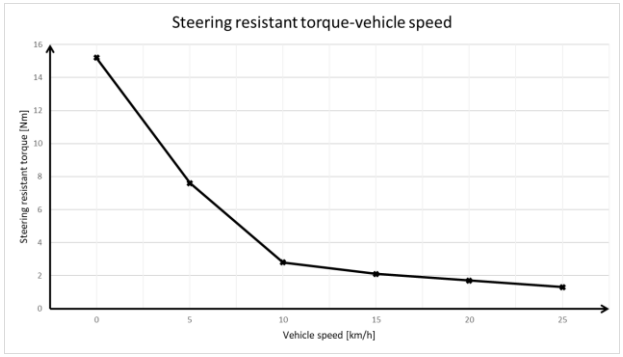

Figure 6. Steering resistant torque as a function of vehicle speed.

$$M_{tire} = \frac{1}{A}\int_A FrdA \tag{5}$$

Where A is the entire contact area.

Because pressure distribution and friction conditions are unknown, measurements were made at different speeds to determine steering torque.

During the measurements, a torque was added on the steering column, the rotation of the steering column was measured at different vehicle speeds. M_{tire} can only be determined if M_{sa} and Θ are already known in (3), because in this case M_{tire} is the only unknown in the equation. M_{sa} has benn determined from Fig. 4, Θ is already known, δ has been measured.

The measurements started from 0 km/h, increasing the speed by 5 km / h in all measurements, up to 25 km / h. "Fig. 6" shows measurement results. The result of the measurements is a steering torque value at the current speed. A linear function has been fitted between all adjacent points, so the torque value between each point can be calculated by linear interpolation.

Knowing these, the dynamic model of the steering system has been created in software environment.

III. Comparison of the Simulation and Measurement Results

After the intended development of the vehicle model has been completed, the simulation can be run. The results are expected to be as close as possible to the real vehicle measurements, but it is not expected that the simulation exactly matches the measurement results. If the simulation results approach the measurement result in nature, then the vehicle model can be considered acceptable, because perfect match will not be realized due to random affect from the environment and inaccuracies in the model. Most important is the presence of a defective form of motion in the simulation, their specific values are not as important because they are significantly influenced by random effects.

In the case of oscillation, the offset from the path and the frequency of the oscillation are the standard basis for comparison. The measured and simulated oscillations need not be in phase.

In the case of overshoot, the place and extent of overshoot is the most important. Even in the case of oscillation and overshoot, their existence is sufficient to draw conclusions about the authenticity of simulation results and, if necessary, further develop the path following controller.

In this chapter the simulation and measurement results are compared. In each figure black line denotes the reference path, green is the recorded path of the vehicle, red is the simulation results of the lateral dynamic bicycle model and blue is the simulation results with the improved dynamic bicycle model, which contains the steering dynamics. . "Table 1." shows the lateral error, it is the mean quadratic error, e_a marks the average lateral error, e_m marks the maximal error.

A. Simulation results – rear wheel position based controller

The simulation results with rear wheel position based controller are shown in Fig. 7, Fig. 8.

In the simulation during the tuning of the controller, the vehicle followed the track accurately, indicated by a red line in Fig 7. In that simulation, the lateral dynamic bicycle model was used.

During the measurements, this controller showed instability, tended to oscillate, especially at higher speed ranges, at 20 km/h the measurement had to be interrupted because the vehicle became dangerously unstable. There was a significant overshoot at cornering maneuvers, as indicated by the green line in Fig. 8.

In the simulation with improved model, which contains the dynamics of steering, the simulation results show the same motion forms, than the measurements. The oscillation is exactly the same, its frequency, amplitude and phase are coincide with the measurement results. The simulation is really close the measurement results. By increasing the speed, the vehicle became unstable in the same way as during the measurements.

Further results are shown in Fig. 7, this illustrates the results of overshoot. The improved vehicle model simulates the overshoot more accurate, the result are significantly closer to the measurement results. The overshoot also appears in the simpler model, but it is less than measured.

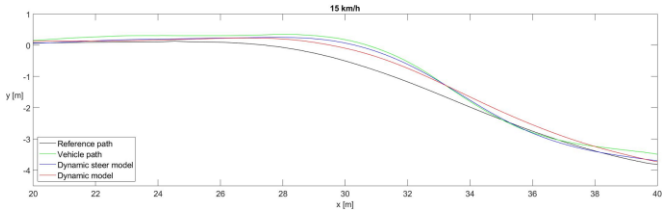

Figure 7. Rear wheel position based controller – small s-curve results at 15 km/h.

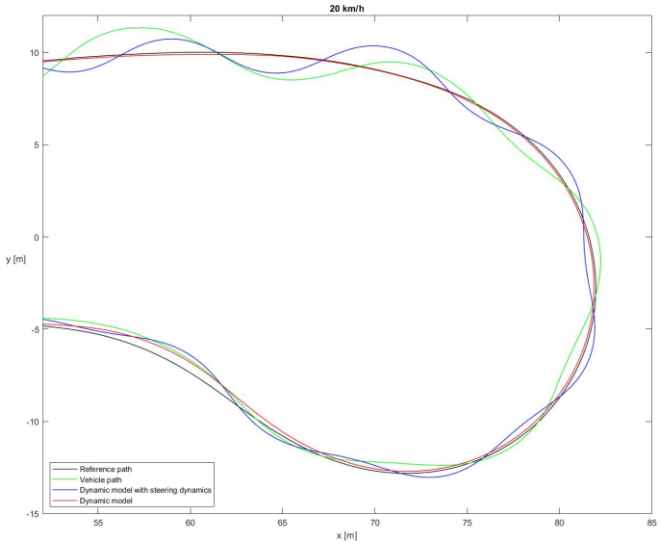

Figure 8. Rear wheel position based controller – reversing curve results at 20 km/h.

The simulation results confirm the measurement results, the upper limit of the rear wheel position based controller applicability is 15 km/h. The controller is tuned to the simpler model, so re-tuning it on the improved model can improve its performance, maximize its usability. This also applies to the other regulators discussed here.

B. *Pure pursuit controller*

The simulation results with pure pursuit controller are shown in Fig. 9 and Fig 10.

With the pure pursuit controller, the improved model also returns the results more accurately. Oscillation is present, its frequency is accurately reproduced by the simulation, but the amplitude is less accurate in the simulation. The overshoot is present, its degree in the simulation is exaggerated.

The simulation results with the improved vehicle model support the measurement results regarding the applicability limits of the pure pursuit controller, its upper limit is 20 km/h.

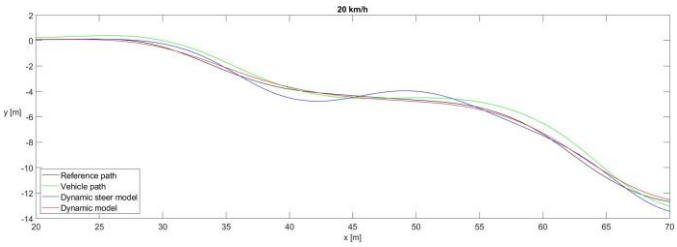

Figure 9. Pure pursuit controller – small s-curve results at 20 km/h.

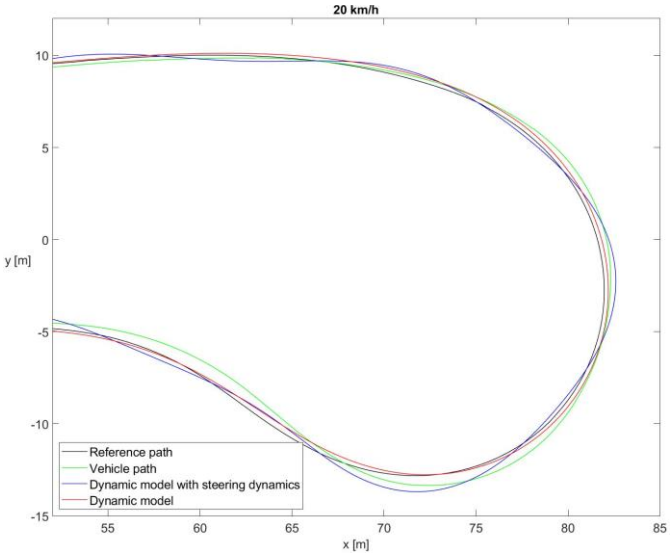

Figure 10. Pure pursuit controller – reversing curve results at 20 km/h.

C. *Front wheel position based controller*

The simulation results with pure pursuit controller are shown in Fig. 11 and Fig. 12.

The oscillation appears in the simulation, its frequency approximating to the measurement results. Overshoot in the simulation with the improved model is closer to the measurement results than the old model.

Based on the simulation results, the applicability limit of the front wheel position based controller is the same as based on the measurement results, its upper limit is 20 km/h.

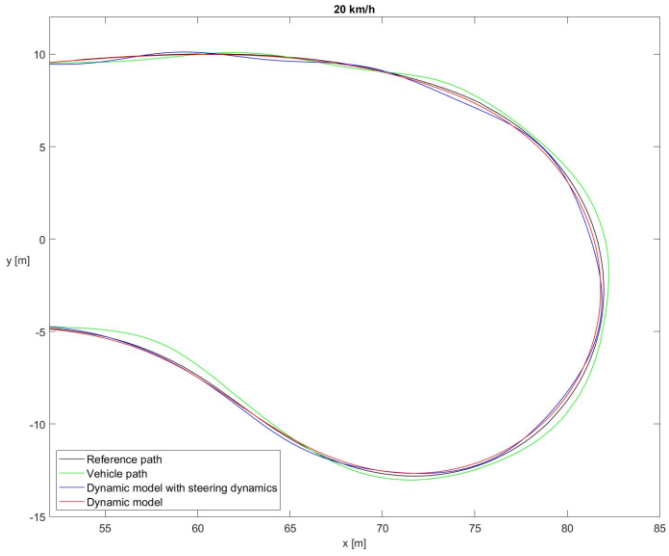

Figure 11. Front wheel position based controller – reversing curve results at 20 km/h.

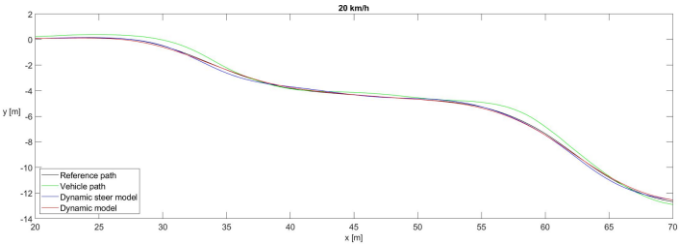

Figure 12. Front wheel position based controller – small s-curve results at 20 km/h.

TABLE I. LATERAL ERROR – 20 KM/H

	Error [m]	Measurement	Dynamic model	Dynamic model with steering dynamics
Pure pursuit	***e_a***	0.3545	0.0890	0.1604
	e_m	0.8927	0.2561	0.8704
Rear whell poision based	***e_a***	0.5288	0.1361	0.6194
	e_m	2.4400	0.5898	2.1141
Front whell poision based	***e_a***	0.2660	0.1000	0.2172
	e_m	0.6235	0.4688	0.5338

IV. CONCLUSION

In this article, the vehicle model used in the previous article by the authors has been developed. The previous model contained only a part of the vehicle's lateral dynamics. Using this model, there were significant differences between measurements and simulation results. Simulation results based on this model are only reliable up to 15 km/h.

Therefore, the model has been further developed, taking into account the dynamic behavior of steering system and tires. The results with the improved vehicle model were close to the measurement results, thus extending the applicability of the simulation to a speed of at least 20 km/h. The model of steering system has been described, measurements have been made to identify the system, its inertia has been determined. A relationship has been established between vehicle speed and tire resistant torque.

With the improved model, the simulations were performed. Finally, the simulation results have been compared, the results were evaluated and showed good correlation with the measurements.

ACKNOWLEDGMENT

The project has been supported by the European Union, co-financed by the European Social Fund. EFOP-3.6.2-16-2017-00002.

REFERENCES

[1] M. Zöldy, “Legal Barriers of Utilization of Autonomous Vehicles as Part of Green Mobility”, Proceedings of the 4th International Congress of Automotive and Transport Engineering (AMMA 2018), 2018.

[2] Á. Nyerges, Z. Szalay, “A new approach for the testing and validation of connected and automated vehicles” pp. 111-114. , 4 p. In: B. Vehovszky, J. Takács, K. Bán (szerk.) 34th International Colloquium on Advanced Manufacturing and Repairing Technologies in Vehicle Industry Budapest, Hungary: Budapest University of Technology and Economics, (2017) p. 190

[3] H. Lengyel, Zs. Szalay, „The Significance and Effect of the Traffic System Signaling to the Environment, Present and Future Traffic”, Proceedings of the 4th International Congress of Automotive and Transport Engineering, pp. 847-856, January 2019.

[4] Á. Domina, V. Tihanyi, "Comparison of path following controllers for autonomous vehicles", SAMI 2019 IEEE 17th World Symposium on Applied Machine Intelligence and Informatics, 2019.

[5] S.Bacha, M.Y.Ayad, R.Saadi, A.Aboubou, M.Bahri, M.Becherif, “Modeling and control technics for autonomous electric and hybrid vehicles path following”, 5th International Conference on Electric Engineering – Boumerdes, 2017.

[6] Á. Bárdos, S. Vass, Á. Nyerges, V. Tihanyi, Z. Szalay, “Path tracking controller for automated driving” pp. 9-12. , 4 p. In: Vehovszky, B; Takács, J; Bán, K (szerk.) 34th International Colloquium on Advanced Manufacturing and Repairing Technologies in Vehicle Industry Budapest, Magyarország : Budapest University of Technology and Economics, (2017) p. 190

[7] B. Paden, M. Cap, S. Z. Yong, D. Yershov, and E. Frazzoli, “A survey of motion planning and control techniques for self-driving urban vehicles”, IEEE Transactions on Intelligent Vehicles, vol. 1, pp. 33-55, June 2016.

[8] S. Bacha, R. Saadi, M. Y. Ayad, A. Aboubou, M. Bahri, “A review on vehicle modeling and control technics used for autonomous vehicle path following”, International Conference on Green Energy Conversion Systems, Busan, 2017.

[9] N. Wu, W. Huang, Z. Song, X. Wu, Q. Zhang, S. Yao, “Adaptive Dynamic Preview Control for Autonomous Vehicle Trajectory Following with DDP Based Path Planner”, IEEE Intelligent Vehicles Symposium, Seoul, June 28-July 1, 2015.

[10] M. Cibooglu, U. Karapmar, M. T. Söylemez, “Hybrid Controller Approach for an Autonomous Ground Vehicle Path Tracking Problem”, 25th Mediterranean Conference on Control and Automation, Valletta, July 2017.

[11] B. Zhang, G. Chen, C. Zong, “Path Tracking of Full Drive-by-Wire Electric Vehicle based on Model Prediction Control”, IEEE Intelligent Vehicles Symposium, Suzuhou, June, 2018.

[12] X. Liu, D. Cebon, “A Minimum Swept Path Control Strategy for Reversing Articulated Vehicles”, IEEE Intelligent Vehicles Symposium, Suzhou, June, 2018.

[13] M. Reiter, D. Abel, “Two and a Half Carrots – A Versatile and Intuitive Optimisation-Based Paath-Following Approach for Road Vehicles”, 23rd Mediterranean Conference on Control and Automation, Valletta, Torremolinos, June 2015.

[14] M. Dai, J. Wang, N. Chen, G. Yin, “Fuzzy steering assistance control for path following of the steer-by-wire vehicle considering characteristics of human driver”, IEEE Intelligent Vehicles Symposium, Suzhou, June, 2018.

[15] J. Ni, J, Hu, “Path Following Control for Autonomous Formula Racecar: Autonomous Formula Student Competition”, IEEE Intelligent Vehicles Symposium, Redondo, June, 2017.

[16] C. Kim, M. Kim, K. Lee, H. Jang, T. S. Park, “Development of a Full Speed Range Path-following System for the Autonomous Vehicle”, 15th International Conference on Control, Automation and Systems, Oct. 2015.

[17] W. ChunYan, Z. YuQi, Z. WanZhong, “Multi-objective optimization of a steering system considering steering modality”, *Advances in Engineering Software*, vol. 126, pp. 61-74, 2018.

[18] R. N. Jazar, *Vehicle Dynamics: Theory and Application.* Springer, 2008.

[19] G. Rill, *Vehicle Dynamics.* Fachhochschule Regensburg, University of Applied Sciences, August 2007.

[20] A. Vijay Alagappan, K.V. Narasimha Rae, “A comparison of various algorithms to extract Magic Formula tyre model coefficients for vehicle dynamics simulations”, Vehicle System Dynamics: International Journal of Vehicle Mechanics and Mobility, February 2015.